

### Unitary group approach to the treatment of mixed-orbital configurations

R. D. Kent and M. Schlesinger

Department of Physics, University of Windsor, Windsor, Ontario, Canada N9B 3P4

(Received 16 July 1980)

Recent advances in the unitary group, or Weyl tableau, approach to the theory of complex spectra have provided great simplification of calculations in atomic and molecular applications. We show that the subduction coefficients employed by Patterson and Harter to generate mixed-orbital-configuration  $LS$ -adapted states can be derived using simple vector-coupling considerations. Using lowering and projection operator techniques based on the idea of "highest tableau," which we show are automatically eigenstates of the  $L^2$  operator, we generate equivalent states. These states are used to calculate reduced matrix elements of the spin-own-orbit operator for the case  ${}^2(p^2d)$ . We discuss the generalization of the existing minicomputer programs to treat mixed-orbital configurations.

#### I. INTRODUCTION

In recent years a great deal of progress has been made in the implementation of unitary-group methods to atomic and molecular problems.<sup>1-3</sup> This has greatly reduced the complexity of calculations in atomic and molecular many-body problems. In this paper we work out detailed expressions and discuss the minicomputer implementation of the unitary-group approach to the case of mixed-orbital configurations in atoms.

An extension like this proves difficult using the traditional Racah scheme. First, the labeling of states in terms of  $L$  and seniority numbers for  $f^5$  electrons and beyond, even in pure configuration, breaks down. Second, difficulties arise due to expressions involving  $3n-j$  and fractional parentage coefficients. The latter have no closed form expressions. This fact requires the storage of large "look up" tables making a minicomputer implementation all but impossible.

Patterson and Harter (PH) (Ref. 4) have recently discussed the generation and classification of mixed configuration states in terms of breaking the corresponding group  $U_n$  into its various component product groups, and using  $LS$  labeling based on the concept of parentage.

In the balance of this work we shall, after a brief outline of the theory, show the equivalence of the (PH) method to a standard vector coupling approach. Next, we shall show that from the point of view of computer implementation, the equivalent lowering-projection operator technique<sup>1</sup> [Drake, Drake, and Schlesinger (DDS)] is to be preferred. Last, we give a sample calculation of reduced matrix elements of the spin-own-orbit operator between states of  ${}^2(p^2d)$ .

#### II. OUTLINE OF THEORY

##### A. Pure orbital configurations

A completely antisymmetric  $N$  electron state will be represented by the product of a two column

Weyl tableau (see Fig. 1) with boxes labeling the one electron orbital quantum numbers of the electrons, and a conjugate two-row tableau with boxes labeling the corresponding one electron spin quantum numbers. The product of orbital and spin tableau uniquely define the vector  $|l^N S M_L M_S; (\alpha)\rangle$ , where  $l$  denotes the orbital angular momentum of a single electron,  $S$  the resultant spin, and  $M_L$  and  $M_S$  the resultant orbital and spin projections, i.e.,

$$M_L = \sum_{i=1}^N m_{l,i} = N(l+1) - \sum_{i=1}^a \alpha_i^- - \sum_{i=1}^b \alpha_i^+, \quad (2.1)$$

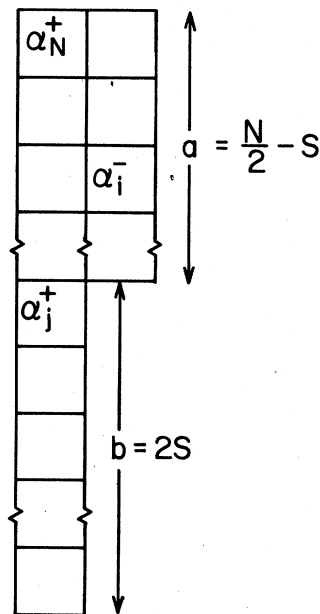


FIG. 1. Tableau labeling: Lexical tableaux are defined by the properties that each  $\alpha_i^+$  is less than or equal to the value  $\alpha_j^+$  in the box to its right and each  $\alpha_i^+$  is less than the value  $\alpha_j^+$  in the box below it. Indexing is defined so that the maximum  $\alpha_i^+ = \alpha_1$ , the next largest  $\alpha_2$ , and so on, to the minimum  $\alpha_N$  which is always located in the upper left column box.

$$M_S = \sum_{i=1}^N m_{s,i} \tag{2.2}$$

For a given tableau ( $\alpha$ ) shape it is clear that there can only be one tableau of highest  $M_L$ , namely the one which contains  $\alpha_i$ , having the lowest allowed lexical values. Hence, we shall have with  $\alpha_i^* = i$ ,

$$M_L(\max) = (2a + b)(l + 1) - \frac{a(a + 1)}{2} - \frac{(a + b)(a + b + 1)}{2} \tag{2.3}$$

In order to generate definite  $L$ -labeled states, we begin by defining the highest  $M_L(\max)$  labeled tableau as

$$|l^N L_{\max} S M_L(\max) M_S\rangle = |l^N S M_L(\max) M_S; (\alpha)\rangle \tag{2.4}$$

Next we proceed, in the fashion described by DDS,<sup>1</sup> by successive application of the lowering operator  $L_{-1}$ . We shall be able to generate all  $|L_{\max}, M_L\rangle$  labeled states. The remaining  $L < L_{\max}$  labeled states can be generated by a projection operator technique and each in turn is then lowered using  $L_{-1}$  until all  $L$ -labeled states corresponding to a given tableau shape have been generated. When several states of the same  $L$  are present at a given  $M_L$  level, an extra quantum number is chosen (such as seniority, although this alone does not suffice for the case of  $f^5$  and beyond).

**B. Mixed orbital configurations**

When a given electron can occupy any of  $t$  different orbitals  $l_1, l_2, \dots, l_t$ , there will be  $n = (2l_1 + 1) + (2l_2 + 1) + \dots + (2l_t + 1)$  states for it. The corresponding  $n^2$  "one-body" operators for these states will generate the group  $U_n = U_{[2(l_1 + \dots + l_t) + t]}$ .

In the case of many electrons, such that  $N_1$  occupy states in the  $l_1$  labeled orbital and  $N_2$  occupy states in the  $l_2$  labeled orbital, etc., we have a mixed orbital configuration denoted by  $(l_1^{N_1})(l_2^{N_2}) \dots (l_t^{N_t})$  with  $N = N_1 + N_2 + \dots + N_t$ . Here, too, we consider the group  $U_{[2(l_1 + l_2 + \dots + l_t) + t]}$  and we choose tableau box labels  $\alpha_i$  such that for the  $j$ th pure configuration  $l_j^{N_j}$

$$2(l_1 + \dots + l_{j-1}) + j \leq \alpha_i^{(j)} \leq 2(l_1 + \dots + l_j) + j \tag{2.5}$$

$$|({}^{2S^{(1)}+1}l_1^{N_1}l_2^{N_2} \dots l_t^{N_t})_2 S_i M_{S,i}\rangle = \sum_{S_{i-1}^{(2)}} [(2S_{i-1} + 1)(2S_i^{(2)} + 1)]^{1/2} (-1)^{S^{(1)} + S_{i-1}^{(2)} + S_i + 1/2} \begin{pmatrix} S^{(1)} & S_{i-1}^{(2)} & S_{i-1} \\ \frac{1}{2} & S_i & S_i^{(2)} \end{pmatrix} \times |({}^{2S^{(1)}+1}l_1^{N_1})({}^{2S^{(2)}+1}l_2^{N_2}) S_i M_{S,i}\rangle \tag{3.1}$$

The vector coupling coefficients in (3.1) have four possible values which we list below.

We can now select families of tableaux corresponding to  $l_1^N, l_1^{N-1}l_2, \dots, l_1^{N_1}l_2^{N_2} \dots l_t^{N_t}, \dots, l_t^N$ . Each of these families corresponds to a particular mixed orbital configuration subgroup of  $U_{[2(l_1 + \dots + l_t)]}$ .

When we couple the conjugate spin tableaux, we can then define the subgroups  $({}^{2S_1+1}l_1^{N_1}) \dots ({}^{2S_t+1}l_t^{N_t})$  of  ${}^{2S+1}(l_1 \dots l_t)^N$ . The next task is that of calculating  $L$ -adapted eigenvectors as was done in the case of pure orbital configurations. This can be achieved in two different ways. The one discussed by Patterson and Harter [(PH) (Ref. 4)] uses so-called subduction coefficients to couple parent configuration defined  $L$ -labeled vectors of the groups  $U_{[l_1]} \times U_{[l_2]} \times \dots \times U_{[l_t]}$  ( $[l] = 2l + 1$ ).

The other approach, suggested by us (Ref. 1) for pure orbital configurations is that of using lowering and projection operators to obtain  $L$  adapted vectors from a highest  $L$  state tableau (highest tableau).

In what follows, we shall first show that the rules stated by PH for the derivation of the subduction coefficients can easily be derived from standard vector coupling or a simple application of graphical methods of angular momentum analysis. Second, we clarify certain ambiguities regarding the lowering operator method<sup>1,4</sup> and show it to be suitable for computer implementation.

**III. EQUIVALENCE OF SUBDUCTION METHOD TO VECTOR COUPLING APPROACH**

We shall restrict our discussion to the case of two pure configurations  $l_1^{N_1}$  and  $l_2^{N_2}$  coupling to give mixed states  $l_1^{N_1}l_2^{N_2}$ . The extension to  $t$ -mixed configurations is straightforward as we shall show below.

The coupling of spin and orbital tableaux can be performed in two different ways. We can begin with a pure configuration tableau state  $|l_1^{N_1} S^{(1)} M_L^{(1)} M_S^{(1)}; (\alpha^{(1)})\rangle$  and we can successively couple  $l_2$ -labeled electrons onto this parent state arriving after adding  $i$  electrons at the state  $|{}^{2S^{(1)}+1}l_1^{N_1}l_2^i S_i M_{L,i} M_{S,i}\rangle$ .

We could have also proceeded by coupling all  $l_2$ -labeled electrons together and then coupling the pure configuration states together to give  $|e^{S^{(1)}+1}l_1^{N_1}({}^{2S_i^{(2)}+1}l_2^i) S_i M_{L,i} M_{S,i}\rangle$ . These are equivalent. In fact, we can write [Brink and Satchler (BS), 1968] (Ref. 5)

Case A:  $S_i = S_{i-1} + \frac{1}{2}$ ,  $S_i^{(2)} = S_{i-1}^{(2)} + \frac{1}{2}$ ,

$$(-1)^{2S_{i-1}} \left( \frac{(S_i + S_i^{(2)} - S^{(1)})(S^{(1)} + S_i + S_i^{(2)} + 1)}{(2S_i + 1)(2S_i^{(2)})} \right)^{1/2}$$

Case B:  $S_i = S_{i-1} - \frac{1}{2}$ ,  $S_i^{(2)} = S_{i-1}^{(2)} + \frac{1}{2}$ ,

$$(-1)^{2S_i} \left( \frac{(S^{(1)} + S_i^{(2)} - S_i)(S^{(1)} + S_i - S_i^{(2)} + 1)}{(2S_i + 1)(2S_i^{(2)})} \right)^{1/2}$$

Case C:  $S_i = S_{i-1} + \frac{1}{2}$ ,  $S_i^{(2)} = S_{i-1}^{(2)} - \frac{1}{2}$ ,

$$(-1)^{2S_{i-1}} \left( \frac{(S^{(1)} + S_i^{(2)} - S_i + 1)(S^{(1)} + S_i - S_i^{(2)})}{(2S_i + 1)(2S_i^{(2)} + 2)} \right)^{1/2}$$

Case D:  $S_i = S_{i-1} - \frac{1}{2}$ ,  $S_i^{(2)} = S_{i-1}^{(2)} - \frac{1}{2}$ ,

$$(-1)^{2S_i} \left( \frac{(S^{(1)} + S_i^{(2)} + S_i + 2)(S_i^{(2)} + S_i - S^{(1)} + 1)}{(2S_i + 1)(2S_i^{(2)} + 2)} \right)^{1/2}$$

The cases A-D above correspond to the cases A-D of PH (1977).<sup>4</sup> The remaining case E of PH corresponds to the coupling of a pair of electrons having the same  $m_l$  values. Here, we find

$$|(l_1^{N_1} l_2^{N_2})^2 S_i M_{S_i}\rangle = \sum_{s_{i-2}^{(2)}} [(2S_{i-2} + 1)(2S_i^{(2)} + 1)]^{1/2} \times (-1)^{S^{(1)} + S_i + s_{i-2}^{(2)}} \begin{Bmatrix} S^{(1)} & S_{i-2}^{(2)} & S_{i-2} \\ 0 & S_i & S_i^{(2)} \end{Bmatrix} \times |(l_1^{N_1})(l_2^{N_2}) S_i M_{S_i}\rangle. \quad (3.2)$$

The coefficients here have the following form.

Case E:  $\delta(S_i, S_{i-2})\delta(S_i^{(2)}, S_{i-2}^{(2)})$ . The difference in phases between the vector coupling approach and the method of PH is accounted for by Drake and Schlesinger [DS 1977].

The equivalence of Eqs. (3.1) and (3.2) to Patterson and Harter's subduction coefficients used in defining definite  $L$ -labeled states constitutes a proof of their method; it should be stressed as it contributes greatly to one's understanding of the tableau formalism for mixed configurations.

Finally, it is also clear in this context how to proceed with the case of more general mixed configurations. If we consider, for example,  $({}^{2S^{(1)}+1}l_1^{N_1})({}^{2S^{(2)}+1}l_2^{N_2})$  coupled to  $({}^{2S_i^{(3)}}l_3^{N_3})$  and  $(l_3)$  then we can define states

$$| \{ [({}^{2S^{(1)}+1}l_1^{N_1})({}^{2S^{(2)}+1}l_2^{N_2})]({}^{2S_i^{(3)}}l_3^{N_3}) \} l_3 S_i M_{S_i} \rangle,$$

$$| [({}^{2S^{(1)}+1}l_1^{N_1})({}^{2S^{(2)}+1}l_2^{N_2})]({}^{2S_i^{(3)}}l_3^{N_3}) S_i M_{S_i} \rangle,$$

$$| \{ ({}^{2S^{(1)}+1}l_1^{N_1}) [({}^{2S^{(2)}+1}l_2^{N_2})({}^{2S_i^{(3)}}l_3^{N_3})] \} S_i M_{S_i} \rangle,$$

and so on. The relationships between these various equivalent representations is displayed (Brink and Satchler) using  $9-j$  symbols.

Finally, in Appendix A we derive the same results for the coupling transformation coefficients using graphical methods of angular momentum analysis.

IV. LOWERING OPERATOR METHOD FOR THE GENERATION OF  $L$ -ADAPTED BASES

A. Pure orbital configurations

In Ref. 1 (DDS) the generation of  $L$ -adapted bases from highest tableaux of pure  $l^N$  configurations was discussed in detail. Briefly, the transformation coefficients from the tableau defined basis  $|l^N SM_L M_S; (\alpha)\rangle$  to the  $L$ -adapted basis  $|l^N LSM_L M_S \tau\rangle$  are generated using the lowering operator

$$L_{-1} = - \sum_{p=1}^N \left( \frac{\alpha'_p(2l+1-\alpha_p)}{2} \right)^{1/2} E(\alpha'_p, \alpha_p), \quad (4.1)$$

where  $\tau$  is any necessary additional quantum number, and  $E(\alpha'_p, \alpha_p)$  represents a sum of single-particle operators  $e_p(\alpha'_p)$  such that

$$e_p(\alpha'_p \alpha_q) |l^{\frac{1}{2}} \alpha_q m_{s,q}\rangle = \delta(p, q) \delta(\alpha'_p, \alpha_q) |l^{\frac{1}{2}} \alpha_p m_{s,p}\rangle. \quad (4.2)$$

$L$ -labeled states not produced through lowering are generated using projection techniques. One can express the transformation coefficients recursively by  $\{\Phi_1[L_{\max}, M_L(\max)1] = 1\}$

$$\Phi_I(LM_L \tau) = - \left( \frac{2}{(L+M_L+1)(L-M_L)} \right)^{1/2} \sum_{I'=1}^{Q_{M_L+1}} \left[ \left( \frac{\alpha'_p(2l+1-\alpha_p)}{2} \right)^{1/2} E_p \right]_{I, I'} \Phi_{I'}(LM_L+1\tau), \quad (4.3)$$

$$\Phi_I(LM_L \tau) = \frac{\delta(L, M_L)}{D} \sum_{\substack{L'=M_L \\ \tau'=M_L}}^{L_{\max}} [\delta(I, \tau) - \Phi_I(L'M_L \tau') \Phi_{\tau'}(L'M_L \tau')], \quad (4.4)$$

where  $E_p$  is the matrix element of the  $E(\alpha'_p, \alpha_p)$  operator between the  $I'$ th tableau at level  $M_L+1$  and the  $I$ th tableau at level  $M_L$ ,  $Q_{M_L+1}$  is the number of tableaux at level  $M_L+1$ , and  $D$  is a normalization factor. The label  $\tau$  is chosen in this method so as to distinguish between the different same- $L$  vectors at the same  $M_L$  level. The transformation between  $L$ -adapted and tableau states is then written as

$$|l^N LSM_L M_S \tau\rangle = \sum_{I=1}^{Q_{M_L}} \Phi_I(LM_L \tau) |l^N SM_L M_S; (\alpha)\rangle_I, \quad (4.5)$$

where the  $\Phi_I(LM_L \tau)$  satisfy the orthonormality conditions

$$\sum_{I=1}^{Q_{M_L}} \Phi_I(LM_L \tau) \Phi_I(L'M_L \tau') = \delta(L, L') \delta(\tau, \tau'). \quad (4.6)$$

B. Mixed orbital configuration

In the case of mixed configurations the procedure is entirely analogous. A complete basis set of operators for the group  $U_n$  is given in terms of irreducible tensor operators by

$$V_q^k(l_r l_t) = \sum_{i,j} (-1)^{i_r+i_t-m'_{r,i}-m'_{t,j}} (2k+1)^{1/2} \begin{pmatrix} l'_r & k & l_t \\ -m'_{r,i} & q & m_{t,j} \end{pmatrix} E(m'_{r,i}, m_{t,j}), \quad (4.7)$$

where  $r, t$  denote the  $r$ th and  $t$ th pure configurations ( $l_r^N r$ ) and ( $l_t^N t$ ). Using (4.7) we can define intrashell ( $l_r=l_t; r=t$ ) and intershell ( $l_r \neq l_t$ ) operators. In particular, we define the orbital operators by

$$L_{-1} = \sum_{p=1}^N (-1)^{l_p-m'_{1,p}} [l_p(l_p+1)(2l_p+1)]^{1/2} \begin{pmatrix} l_p & 1 & l_p \\ -m'_{1,p} & 1 & m_{1,p} \end{pmatrix} E(\alpha'_p, \alpha_p) \\ = - \sum_{p=1}^N \left( \frac{\alpha'_p(2l_p+1-\alpha'_p)}{2} \right)^{1/2} E(\alpha'_p, \alpha_p) \quad (4.8)$$

and

$$L_0 = \sum_{p=1}^N (l_p+1-\alpha'_p) E(\alpha'_p, \alpha_p). \quad (4.9)$$

The operator  $L_{+1}$  is similar to (4.8), involving a change of overall sign and interchange of primes

and no primes on the  $\alpha$ 's. With  $N=N_1+N_2+\dots$  one sees by comparing (4.8) with (4.1) that the form of the operators is the same for mixed and pure configurations requiring, of course, that  $l$

be labeled for the  $p$ th electron in the mixed orbital case.

The generation of vectors at a given  $M_L$  level, having the same  $L$ , is again accomplished by a projection technique and the transformation coefficients  $\Phi_r(LM_L\tau)$  are defined by (4.3) and (4.4).

The use of lowering and projection techniques in the generation of  $L$ -adapted bases for pure or mixed orbital configurations depends on being able to have at least one eigenvector of definite  $L$ . In the pure orbital configuration case this choice is immediate, since for  $M_L(\max)$  there exists only one tableau state and this defines an  $L_{\max}$ -labeled state. In the case of mixed orbital configurations this situation may not always occur. In other words, several "highest tableaux" [defined as all lexical tableaux of the configuration that cannot be raised by any intrashell operator  $E(\alpha_p, \alpha'_p)$ ] may exist for a given configuration. We show in Appendix B, however, that each of these highest tableaux is, in fact, an eigenvector of definite  $L$ , and consequently the states of a mixed orbital configuration will be found by systematically lowering the highest tableaux just as one does for a pure orbital configuration.

#### V. APPLICATION TO SPIN-OWN-ORBIT MATRIX ELEMENTS

In this section we demonstrate a calculation of the spin-own-orbit matrix elements for mixed orbital configurations. For our example we consider the case of  ${}^2(p^2d)$  which we split into two families,  ${}^2[({}^1p^2)d]$  and  ${}^2[({}^3p^2)d]$ .

Numbering  $p$ - and  $d$ -labeled boxes by  $\alpha = 1, \dots, 3$  and  $\alpha = 4, \dots, 8$ , respectively, we find for highest tableaux the states

$$|({}^1p^2)dL = 4S = \frac{1}{2}M_L = 4M_S\rangle = \left| \begin{array}{|c|c|} \hline 1 & 1 \\ \hline 4 & \\ \hline \end{array} \right\rangle_{M_S}, \quad (5.1)$$

$$|({}^3p^2)dL = 3S = \frac{1}{2}M_L = 3M_S\rangle = \left| \begin{array}{|c|c|} \hline 1 & 4 \\ \hline 2 & \\ \hline \end{array} \right\rangle_{M_S}. \quad (5.2)$$

The remaining tableaux generated from these highest tableaux are given in Tables I and II. The superscripts on each tableau are index labels I to be used in conjunction with the transformation coefficients defined in (4.3) and Tables III and IV. These last two tables are generated using the lowering and projection operator techniques defined in equations (4.1) and (4.8).

The spin-own-orbit operator is defined by<sup>3</sup>

$$V_{SO} = \sum_{\gamma=-1}^1 (-1)^{-\gamma} \sum_{i=1}^N l_{i,-\gamma} S_{i,\gamma}, \quad (5.3)$$

where  $l_{i,-\gamma}$  and  $S_{i,\gamma}$  are single-particle orbital and spin operators which can be expressed in

TABLE I. Tableau states of  ${}^2[({}^1p^2)d]$ .

$M_L$	$Q_{M_L}$	(Tableau) <sup>I</sup>
4	1	$\begin{array}{ c c } \hline 1 & 1 \\ \hline 4 & \\ \hline \end{array}^1$
3	2	$\begin{array}{ c c } \hline 1 & 1 \\ \hline 5 & \\ \hline \end{array}^1 \begin{array}{ c c } \hline 1 & 2 \\ \hline 4 & \\ \hline \end{array}^2$
2	4	$\begin{array}{ c c } \hline 1 & 1 \\ \hline 6 & \\ \hline \end{array}^1 \begin{array}{ c c } \hline 1 & 2 \\ \hline 5 & \\ \hline \end{array}^2 \begin{array}{ c c } \hline 2 & 2 \\ \hline 4 & \\ \hline \end{array}^3 \begin{array}{ c c } \hline 1 & 3 \\ \hline 4 & \\ \hline \end{array}^4$
1	5	$\begin{array}{ c c } \hline 1 & 1 \\ \hline 7 & \\ \hline \end{array}^1 \begin{array}{ c c } \hline 1 & 2 \\ \hline 6 & \\ \hline \end{array}^2 \begin{array}{ c c } \hline 2 & 2 \\ \hline 5 & \\ \hline \end{array}^3 \begin{array}{ c c } \hline 1 & 3 \\ \hline 5 & \\ \hline \end{array}^4 \begin{array}{ c c } \hline 2 & 3 \\ \hline 4 & \\ \hline \end{array}^5$
0	6	$\begin{array}{ c c } \hline 1 & 1 \\ \hline 8 & \\ \hline \end{array}^1 \begin{array}{ c c } \hline 1 & 2 \\ \hline 7 & \\ \hline \end{array}^2 \begin{array}{ c c } \hline 2 & 2 \\ \hline 6 & \\ \hline \end{array}^3 \begin{array}{ c c } \hline 1 & 3 \\ \hline 6 & \\ \hline \end{array}^4 \begin{array}{ c c } \hline 2 & 3 \\ \hline 5 & \\ \hline \end{array}^5 \begin{array}{ c c } \hline 3 & 3 \\ \hline 4 & \\ \hline \end{array}^6$
-1	5	$\begin{array}{ c c } \hline 1 & 2 \\ \hline 8 & \\ \hline \end{array}^1 \begin{array}{ c c } \hline 2 & 2 \\ \hline 7 & \\ \hline \end{array}^2 \begin{array}{ c c } \hline 1 & 3 \\ \hline 7 & \\ \hline \end{array}^3 \begin{array}{ c c } \hline 2 & 3 \\ \hline 6 & \\ \hline \end{array}^4 \begin{array}{ c c } \hline 3 & 3 \\ \hline 5 & \\ \hline \end{array}^5$
-2	4	$\begin{array}{ c c } \hline 2 & 2 \\ \hline 8 & \\ \hline \end{array}^1 \begin{array}{ c c } \hline 1 & 3 \\ \hline 8 & \\ \hline \end{array}^2 \begin{array}{ c c } \hline 2 & 3 \\ \hline 7 & \\ \hline \end{array}^3 \begin{array}{ c c } \hline 3 & 3 \\ \hline 6 & \\ \hline \end{array}^4$
-3	2	$\begin{array}{ c c } \hline 2 & 3 \\ \hline 8 & \\ \hline \end{array}^1 \begin{array}{ c c } \hline 3 & 3 \\ \hline 7 & \\ \hline \end{array}^2$
-4	1	$\begin{array}{ c c } \hline 3 & 3 \\ \hline 8 & \\ \hline \end{array}^1$

terms of the irreducible tensor operators  $V_q^k$  defined in (4.7).

The reduced matrix elements of (5.3) in the representation corresponding to the  $|({}^{2S}({}^{1+1}L_1^{N_1}))_{L_2}^{N_2} SM_L M_S; (\alpha)\rangle$  vector's can be written in terms of the cases  $\gamma = 0, -1$  separately.

TABLE II. Tableau states of  ${}^2[({}^3p^2)d]$ .

$M_L$	$Q_{M_L}$	(Tableau) <sup>I</sup>
3	1	$\begin{array}{ c c } \hline 1 & 4 \\ \hline 2 & \\ \hline \end{array}^1$
2	2	$\begin{array}{ c c } \hline 1 & 4 \\ \hline 3 & \\ \hline \end{array}^1 \begin{array}{ c c } \hline 1 & 5 \\ \hline 2 & \\ \hline \end{array}^2$
1	3	$\begin{array}{ c c } \hline 2 & 4 \\ \hline 3 & \\ \hline \end{array}^1 \begin{array}{ c c } \hline 1 & 5 \\ \hline 3 & \\ \hline \end{array}^2 \begin{array}{ c c } \hline 1 & 6 \\ \hline 2 & \\ \hline \end{array}^3$
0	3	$\begin{array}{ c c } \hline 2 & 5 \\ \hline 3 & \\ \hline \end{array}^1 \begin{array}{ c c } \hline 1 & 6 \\ \hline 3 & \\ \hline \end{array}^2 \begin{array}{ c c } \hline 1 & 7 \\ \hline 2 & \\ \hline \end{array}^3$
-1	3	$\begin{array}{ c c } \hline 2 & 6 \\ \hline 3 & \\ \hline \end{array}^1 \begin{array}{ c c } \hline 1 & 7 \\ \hline 3 & \\ \hline \end{array}^2 \begin{array}{ c c } \hline 1 & 8 \\ \hline 2 & \\ \hline \end{array}^3$
-2	2	$\begin{array}{ c c } \hline 2 & 7 \\ \hline 3 & \\ \hline \end{array}^1 \begin{array}{ c c } \hline 1 & 8 \\ \hline 3 & \\ \hline \end{array}^2$
-3	1	$\begin{array}{ c c } \hline 2 & 8 \\ \hline 3 & \\ \hline \end{array}^1$

TABLE III. Transformation coefficients for  $|{}^L p^2 d LSM_L M_S \tau\rangle$  states.

$L(\tau)$	$M_L$	$I =$	$\Phi_I(L M_L \tau)$						
			1	2	3	4	5	6	
4(1)	4		1						
	3		$-\sqrt{\frac{1}{2}}$	$-\sqrt{\frac{1}{2}}$					
	2		$\sqrt{\frac{3}{14}}$	$\sqrt{\frac{4}{7}}$	$\sqrt{\frac{1}{7}}$	$\sqrt{\frac{1}{14}}$			
	1		$-\sqrt{\frac{1}{14}}$	$-\sqrt{\frac{2}{7}}$	$-\sqrt{\frac{2}{7}}$	$-\sqrt{\frac{1}{7}}$	$-\sqrt{\frac{1}{14}}$		
	0		$\sqrt{\frac{1}{70}}$	$\sqrt{\frac{3}{35}}$	$\sqrt{\frac{12}{35}}$	$\sqrt{\frac{6}{35}}$	$\sqrt{\frac{3}{35}}$	$\sqrt{\frac{1}{70}}$	
	-1		$-\sqrt{\frac{1}{14}}$	$-\sqrt{\frac{2}{7}}$	$-\sqrt{\frac{1}{7}}$	$-\sqrt{\frac{3}{7}}$	$-\sqrt{\frac{1}{14}}$		
	-2		$\sqrt{\frac{1}{7}}$	$\sqrt{\frac{1}{14}}$	$\sqrt{\frac{4}{7}}$	$\sqrt{\frac{3}{14}}$			
	-3		$-\sqrt{\frac{1}{2}}$	$-\sqrt{\frac{1}{2}}$					
	-4		1						
3(1)	3		$\sqrt{\frac{1}{2}}$	$-\sqrt{\frac{1}{2}}$					
	2		$-\sqrt{\frac{1}{2}}$	0	$\sqrt{\frac{1}{3}}$	$\sqrt{\frac{1}{6}}$			
	1		$\sqrt{\frac{3}{10}}$	$\sqrt{\frac{1}{5}}$	$-\sqrt{\frac{2}{15}}$	$-\sqrt{\frac{1}{15}}$	$-\sqrt{\frac{3}{10}}$		
	0		$-\sqrt{\frac{1}{10}}$	$-\sqrt{\frac{2}{5}}$	0	0	$\sqrt{\frac{2}{5}}$	$\sqrt{\frac{1}{10}}$	
	-1		$\sqrt{\frac{3}{10}}$	$\sqrt{\frac{2}{15}}$	$\sqrt{\frac{1}{15}}$	$-\sqrt{\frac{1}{5}}$	$-\sqrt{\frac{3}{10}}$		
	-2		$-\sqrt{\frac{1}{3}}$	$-\sqrt{\frac{1}{6}}$	0	$\sqrt{\frac{1}{2}}$			
	-3		$\sqrt{\frac{1}{2}}$	$-\sqrt{\frac{1}{2}}$					
2(1)	2		$\sqrt{\frac{2}{7}}$	$-\sqrt{\frac{3}{7}}$	$\sqrt{\frac{4}{21}}$	$\sqrt{\frac{2}{21}}$			
	1		$-\sqrt{\frac{3}{7}}$	$\sqrt{\frac{1}{14}}$	$\sqrt{\frac{1}{21}}$	$\sqrt{\frac{1}{42}}$	$-\sqrt{\frac{3}{7}}$		
	0		$\sqrt{\frac{2}{7}}$	$\sqrt{\frac{1}{14}}$	$-\sqrt{\frac{4}{21}}$	$-\sqrt{\frac{2}{21}}$	$\sqrt{\frac{1}{14}}$	$\sqrt{\frac{2}{7}}$	
	-1		$-\sqrt{\frac{3}{7}}$	$\sqrt{\frac{1}{21}}$	$\sqrt{\frac{1}{42}}$	$\sqrt{\frac{1}{14}}$	$-\sqrt{\frac{3}{7}}$		
	-2		$\sqrt{\frac{4}{21}}$	$\sqrt{\frac{2}{21}}$	$-\sqrt{\frac{3}{7}}$	$\sqrt{\frac{2}{7}}$			
2(3)	2		0	0	$\sqrt{\frac{1}{3}}$	$-\sqrt{\frac{2}{3}}$			
	1		0	0	$-\sqrt{\frac{1}{3}}$	$\sqrt{\frac{2}{3}}$	0		
	0		0	0	$\sqrt{\frac{1}{3}}$	$-\sqrt{\frac{2}{3}}$	0	0	
	-1		0	$-\sqrt{\frac{1}{3}}$	$-\sqrt{\frac{2}{3}}$	0	0		
	-2		$\sqrt{\frac{1}{3}}$	$-\sqrt{\frac{2}{3}}$					
1(1)	1		$\sqrt{\frac{1}{5}}$	$-\sqrt{\frac{3}{10}}$	$\sqrt{\frac{1}{5}}$	$\sqrt{\frac{1}{10}}$	$-\sqrt{\frac{1}{5}}$		
	0		$-\sqrt{\frac{2}{5}}$	$\sqrt{\frac{1}{10}}$	0	0	$-\sqrt{\frac{1}{10}}$	$\sqrt{\frac{2}{5}}$	
	-1		$\sqrt{\frac{1}{5}}$	$-\sqrt{\frac{1}{5}}$	$-\sqrt{\frac{1}{10}}$	$\sqrt{\frac{3}{10}}$	$-\sqrt{\frac{1}{5}}$		
0(1)	0		$\sqrt{\frac{4}{49}}$	$-\sqrt{\frac{4}{49}}$	$\sqrt{\frac{8}{147}}$	$\sqrt{\frac{4}{147}}$	$-\sqrt{\frac{36}{49}}$	$\sqrt{\frac{1}{49}}$	

Case A:  $\gamma=0 (M'_L=M_L)$ . In this case  $\alpha_i=\alpha'_i (i=1, N)$ . After removing all mutual pairs in our tableaux, we find  $\alpha_i \neq \alpha_j (i \neq j=1, \dots, N)$  and

$$\begin{aligned} & \langle ({}^{2S^{(1)'}+1}L_1^{N_1})L_2^{N_2}S'_0M'_L; (\alpha') \parallel V_{SO} \parallel ({}^{2S^{(1)}+1}L_1^{N_1})L_2^{N_2}S_0M_L; (\alpha) \rangle \\ &= \prod_{i=1}^N \delta(\alpha_i, \alpha'_i) \sum_{p=1}^N \prod_{i \neq p}^N \delta(S_i, S'_i) (l_p+1-\alpha'_p) (-1)^{S_p+S_{p-1}-1/2} \sqrt{\frac{3}{2}} [(2S_{p-1}+1)(2S'_{p-1}+1)]^{1/2} \\ & \quad \times \begin{Bmatrix} S'_{p-1} & S_{p-1} & 1 \\ \frac{1}{2} & \frac{1}{2} & S_p \end{Bmatrix} \prod_{i=0}^{p-2} \bar{M}(i). \end{aligned} \quad (5.4)$$

Case B:  $\gamma=-1 (M'_L=M_L+1)$ . In this case  $\alpha'_i=\alpha_i$  for all  $i$  except  $\alpha'_p=\alpha_p-1$  and

$$\begin{aligned} & \langle ({}^{2S^{(1)'}+1}L_1^{N_1})L_2^{N_2}S'_0M'_L; (\alpha') \parallel V_{SO} \parallel ({}^{2S^{(1)}+1}L_1^{N_1})L_2^{N_2}S_0M_L; (\alpha) \rangle \\ &= \delta(M'_L, M_L+1) \prod_{i=1}^{p-1} \delta(\alpha'_i, \alpha_i) \prod_{i=p+1}^N \delta(\alpha'_i, \alpha_i) \prod_{i=p+1}^N \delta(S'_i S_i) \left( \frac{3\alpha'_p(2L_p+1-\alpha'_p)}{4} \right)^{1/2} \bar{E}_p \prod_{i=0}^{p-3} \bar{M}(i), \end{aligned} \quad (5.5)$$

where

$$\bar{M}(i) = [(2S_i+1)(2S'_i+1)]^{1/2} \begin{Bmatrix} 1 & S'_i & S_i \\ \frac{1}{2} & S_{i+1} & S'_{i+1} \end{Bmatrix} (-1)^{S'_{i+1}+S_i-1/2} \quad (5.6)$$

and  $\bar{M}(-1)=1$ , by definition.

For  $\bar{E}_p$  we find four possible forms, namely,

$$\begin{aligned} \bar{E}_p &= \delta(S_p S'_p) [(2S_{p-1}+1)(2S'_{p-1}+1)]^{1/2} (-1)^{S_p+S_{p-1}-1/2} \begin{Bmatrix} S'_{p-1} & S_{p-1} & 1 \\ \frac{1}{2} & \frac{1}{2} & S_p \end{Bmatrix} \bar{M}(p-2) && \text{if } \alpha_p \neq \alpha_{p-1}, \alpha'_p \neq \alpha'_{p+1}, \\ \bar{E}_p &= \delta(S_p S'_p) \delta(S_p S_{p-2}) (-1)^{2S'_{p-1}+S_{p-2}-S'_p-2} [(2S'_{p-1}+1)(2S'_{p-2}+1)]^{1/2} \begin{Bmatrix} S_{p-2} & S'_{p-2} & 1 \\ \frac{1}{2} & \frac{1}{2} & S'_{p-1} \end{Bmatrix} && (5.7) \\ \bar{E}_p &= \delta(S_p S'_p) (-1)^{2S_p+1} [(2S_p+1)(2S_{p-1}+1)]^{1/2} \begin{Bmatrix} S'_{p-1} & S_{p-1} & 1 \\ \frac{1}{2} & \frac{1}{2} & S_p \end{Bmatrix} \bar{M}(p-2) && \text{if } \alpha_p \neq \alpha_{p-1}, \alpha'_p = \alpha'_{p+1}, \\ \bar{E}_p &= \delta(S_p S_{p-2}) \delta(S'_{p+1} S'_{p-1}) [(2S_{p-2}+1)(2S'_{p-2}+1)]^{1/2} (-1)^{S'_{p-2}+S'_{p-1}-1/2} \begin{Bmatrix} S_{p-2} & S'_{p-2} & 1 \\ \frac{1}{2} & \frac{1}{2} & S'_{p-1} \end{Bmatrix} && \text{if } \alpha_p = \alpha_{p-1}, \alpha'_p = \alpha'_{p+1}. \end{aligned}$$

The counting order of the spin chain ( $S_i$ ) is taken so that  $S_0$  is the total spin,  $S_1$  the spin after removing the highest  $\alpha$  value, and  $S_N=0$  the spin after all boxes have been removed.

The case  $\gamma=1$  is of the same form as case B, interchanging primes and no primes where necessary, and changing the overall sign to minus.

Table V contains values of matrix elements of  $V_{SO}$  between tableau states. Once the computations of the  $V_{SO}$  matrix elements has been completed, the transformation to states of, say, definite  $L$  is quite simple. We write

$$\begin{aligned} & \langle ({}^{2S^{(1)'}+1}L_1^{N_1})L_2^{N_2}L'S'_0M'_L\tau' \parallel V_{SO} \parallel ({}^{2S^{(1)}+1}L_1^{N_1})L_2^{N_2}LSM_L\tau \rangle \\ &= \sum_{\tau'=1}^{Q_{M'_L}} \sum_{\tau=1}^{Q_{M_L}} \Phi_{\tau'}(L'M'_L\tau') \Phi_{\tau}(LM_L\tau) \langle ({}^{2S^{(1)'}+1}L_1^{N_1})L_2^{N_2}S'_0M'_L; (\alpha') I' \parallel V_{SO} \parallel ({}^{2S^{(1)}+1}L_1^{N_1})L_2^{N_2}SM_L; (\alpha) I \rangle, \end{aligned}$$

where the double summation ranges independently over the  $Q_{M'_L}$  and  $Q_{M_L}$  tableaux at levels  $M'_L$  and  $M_L$ , respectively. Further transformation to different labeling schemes, say ( $LSJM_J$ ) labeling, can also be accomplished in a relatively simple manner.

TABLE IV. Transformation coefficients for  $|({}^3p^2)dLSM_L M_S \tau\rangle$  states.

$L(\tau)$	$M_L$	$\Phi_I(LM_L\tau)$			
		$I=$	1	2	3
3(1)	3		1		
	2		$-\sqrt{\frac{1}{3}}$	$-\sqrt{\frac{2}{3}}$	
	1		$\sqrt{\frac{1}{15}}$	$\sqrt{\frac{6}{15}}$	$\sqrt{\frac{2}{5}}$
	0		$-\sqrt{\frac{1}{5}}$	$-\sqrt{\frac{3}{5}}$	$-\sqrt{\frac{1}{5}}$
	-1		$\sqrt{\frac{2}{5}}$	$\sqrt{\frac{8}{15}}$	$\sqrt{\frac{1}{15}}$
	-2		$-\sqrt{\frac{2}{3}}$	$-\sqrt{\frac{1}{3}}$	
	-3		1		
2(1)	2		$\sqrt{\frac{2}{3}}$	$-\sqrt{\frac{1}{3}}$	
	1		$-\sqrt{\frac{1}{3}}$	$-\sqrt{\frac{1}{6}}$	$\sqrt{\frac{1}{2}}$
	0		$\sqrt{\frac{1}{2}}$	0	$-\sqrt{\frac{1}{2}}$
	-1		$-\sqrt{\frac{1}{2}}$	$\sqrt{\frac{1}{6}}$	$\sqrt{\frac{1}{3}}$
	-2		$\sqrt{\frac{1}{3}}$	$-\sqrt{\frac{2}{3}}$	
	-3				
1(1)	1		$\sqrt{\frac{3}{5}}$	$-\sqrt{\frac{3}{10}}$	$\sqrt{\frac{1}{10}}$
	0		$-\sqrt{\frac{3}{10}}$	$\sqrt{\frac{2}{5}}$	$-\sqrt{\frac{3}{10}}$
	-1		$\sqrt{\frac{1}{10}}$	$-\sqrt{\frac{3}{10}}$	$\sqrt{\frac{2}{5}}$

VI. MINICOMPUTER PROGRAMMING CONSIDERATIONS

We have recently<sup>6</sup> completed the minicomputer programming of the generation methods for tableau and  $L$ -adapted bases plus spin-own-orbit reduced matrix element calculations for pure  $l^N$  configurations. The programs were coded in PDP assembler language. They constitute a string of four programs, each less than 20K words (1 word - 16 bits) in length so that a unit of limited memory capacity can handle them sequentially.

The first program, "GENPAL," generates and stores on disk the entire list of tableaux corresponding to a given partition (tableau shape) of the configuration. Optimal storage is achieved by encoding each tableau in terms of a binary string,<sup>2</sup> represented by the expression (cf., Fig. 1)

$$\sum_{i=1}^{n_1} 2^{2\alpha_i - 2} + \sum_{i=1}^d 2^{2\alpha_i - 1}. \tag{6.1}$$

The second program, "ELLMAT," calculates and stores on disk the matrix elements of the  $E(\alpha'_p, \alpha_p)$  operator between two tableaux. The third program, "ZOHAR," uses the output of ELLMAT to compute the transformation coefficients  $\Phi_I(LM_L\tau)$  described in (4.3) and (4.4) which are then stored on disk. At this point, a complete  $L$ -adapted basis is achieved. The final program, "SPNORB," uses the output of GENPAL and ZOHAR to compute reduced matrix elements of the spin-own-orbit operator in the representation of  $|l^N LSM_L \tau\rangle$  vectors. The output of SPNORB can be placed on disk or outputted on a line printer.

In extending the programs to mixed orbital configurations only minor changes need be implemented. In fact, the programs ELLMAT and ZOHAR do not require any changes and SPNORB requires only slight modification to account for differences in state labeling. The only substantial change is in GENPAL, where it becomes necessary to add a program section which accepts the input of specific parent partitions, assigns box labels  $\alpha_i$  corresponding to various  $l$  labels and uniquely constructs a highest tableau. Once this function is performed GENPAL then generates all tableaux according to the algorithm already programmed (for the pure configuration case).

The power of the unitary group approach can be, perhaps, best appreciated by the fact that there is little distinction between pure and mixed orbital configuration treatments. The program batch described above treats both cases effectively.

An additional point should be clarified. The transformation coefficients  $\Phi_I(LM_L\tau)$  and matrix elements of both  $E(\alpha', \alpha)$  and the spin-own-orbit operator can always be calculated in the exact form

$$(-1)^P \sqrt{n/d}, \tag{6.2}$$

where the phase  $P=0, 1$  and  $n$  and  $d$  are integers. In our program we have chosen to utilize this feature to calculate exact values for these various quantities, which we then express in the form (6.2). Using conventional high-level language (e.g., Fortran, Basic, etc.) software overflow can be a problem as the numbers  $n$  and  $d$  can be extremely large [e.g., for the case  ${}^4(f^5)$  configurations  $d$  approaches  $10^{20}$  in some instances]. If one abandons an exact approach and calculates instead the actual numerical value as a decimal number, then significant round-off errors can result.

We have been able to completely overcome these difficulties through the development of arbitrary precision software. In practice, this requires



TABLE V. Spin-own-orbit reduced matrix elements in the tableau representation.

$M_L=4$	$\langle 4^1  $	$  _4^{11}\rangle$	$  _5^{11}\rangle$	$  _4^{12}\rangle$	$  _2^{14}\rangle$											
		$\sqrt{6}$	$\sqrt{3}$	$\cdot$	$1$											
		$M_L=4$				$M_L=3$										
$M_L=3$	$\langle 5^1  $	$  _5^{11}\rangle$	$  _4^{12}\rangle$	$  _2^{14}\rangle$	$  _6^{11}\rangle$	$  _5^{12}\rangle$	$  _4^{22}\rangle$	$  _4^{13}\rangle$	$  _3^{14}\rangle$	$  _2^{15}\rangle$						
		$\sqrt{\frac{3}{2}}$	$\cdot$	$\cdot$	$\sqrt{\frac{3}{2}}$	$\cdot$	$\cdot$	$\cdot$	$\cdot$	$1$						
		$\cdot$	$\sqrt{6}$	$-\sqrt{\frac{1}{2}}$	$\cdot$	$\sqrt{3}$	$\cdot$	$\cdot$	$\sqrt{\frac{1}{2}}$	$\cdot$						
$M_L=3$	$\langle 4^2  $	$\cdot$	$\sqrt{6}$	$-\sqrt{\frac{1}{2}}$	$\cdot$	$\sqrt{3}$	$\cdot$	$\cdot$	$\sqrt{\frac{1}{2}}$	$\cdot$						
		$\cdot$	$-\sqrt{\frac{1}{2}}$	$\cdot$	$\cdot$	$\cdot$	$1$	$-\sqrt{\frac{1}{2}}$	$\sqrt{\frac{2}{3}}$	$-\sqrt{\frac{1}{3}}$						
		$\cdot$	$-\sqrt{\frac{1}{2}}$	$\cdot$	$\cdot$	$\cdot$	$1$	$-\sqrt{\frac{1}{2}}$	$\sqrt{\frac{2}{3}}$	$-\sqrt{\frac{1}{3}}$						
		$M_L=3$				$M_L=2$										
$M_L=2$	$\langle 6^1  $	$  _6^{11}\rangle$	$  _5^{12}\rangle$	$  _4^{22}\rangle$	$  _4^{13}\rangle$	$  _3^{14}\rangle$	$  _2^{15}\rangle$	$  _7^{11}\rangle$	$  _6^{12}\rangle$	$  _5^{22}\rangle$	$  _5^{13}\rangle$	$  _2^{23}\rangle$	$  _3^{24}\rangle$	$  _3^{15}\rangle$	$  _2^{16}\rangle$	
		$\cdot$	$\cdot$	$\cdot$	$\cdot$	$\cdot$	$\cdot$	$\sqrt{\frac{3}{2}}$	$\cdot$	$\cdot$	$\cdot$	$\cdot$	$\cdot$	$\cdot$	$1$	
		$\langle 5^2  $	$\cdot$	$\sqrt{\frac{3}{2}}$	$\cdot$	$\cdot$	$\cdot$	$-\sqrt{\frac{1}{2}}$	$\cdot$	$\sqrt{\frac{3}{2}}$	$\cdot$	$\cdot$	$\cdot$	$\cdot$	$\sqrt{\frac{1}{2}}$	$\cdot$
		$\langle 4^2  $	$\cdot$	$\cdot$	$\sqrt{6}$	$\cdot$	$\cdot$	$\cdot$	$\cdot$	$\cdot$	$\sqrt{3}$	$\cdot$	$\cdot$	$1$	$\cdot$	$\cdot$
		$\langle 4^3  $	$\cdot$	$\cdot$	$\cdot$	$\sqrt{6}$	$-\sqrt{2}$	$\cdot$	$\cdot$	$\cdot$	$\cdot$	$\sqrt{3}$	$\sqrt{\frac{1}{2}}$	$-\sqrt{\frac{1}{2}}$	$\cdot$	$\cdot$
		$\langle 4^4  $	$\cdot$	$\cdot$	$\cdot$	$-\sqrt{2}$	$-\sqrt{\frac{2}{3}}$	$\cdot$	$\cdot$	$\cdot$	$\cdot$	$\cdot$	$\sqrt{\frac{1}{2}}$	$\sqrt{\frac{2}{3}}$	$\sqrt{\frac{1}{3}}$	$\cdot$
$M_L=2$	$\langle 2^5  $	$\cdot$	$-\sqrt{\frac{1}{2}}$	$\cdot$	$\cdot$	$\cdot$	$\sqrt{\frac{1}{6}}$	$\cdot$	$\cdot$	$1$	$-\sqrt{\frac{1}{2}}$	$\cdot$	$\cdot$	$\sqrt{\frac{2}{3}}$	$-\sqrt{\frac{1}{2}}$	
		$M_L=2$				$M_L=1$										

several words of storage for large numbers, but presents only minor problems in programming, each of a bookkeeping nature. The main problem associated with the use of multiple precision software of any type is a significant increase in the time of calculations. Even so, for our computer typical run times for ZOHAR amount to a few hours for very large dimension cases and of the order of  $\approx 10$  h for the spin-own-orbit (SPNORB) calculations. However, our hardware functions are quite slow ( $\sim 5$   $\mu$ sec/operation), as is the case for most minicomputers. By, say, programming in IBM assembler and running on a full-scale computer, we can expect to cut these times very significantly.

#### ACKNOWLEDGMENTS

We wish to acknowledge with thanks many illuminating discussions with Dr. G.W.F. Drake of this department. This research was supported by the Natural Sciences and Engineering Research Council of Canada.

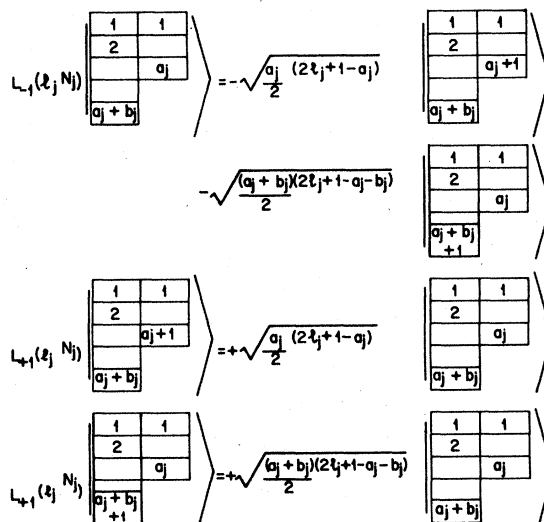
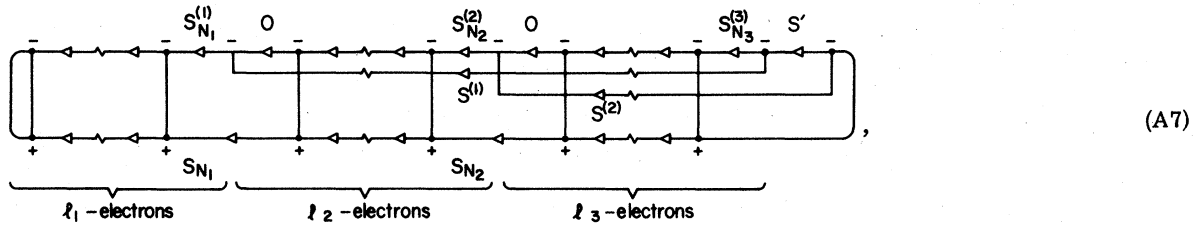


FIG. 2. Raising and lowering of highest tableaux.



ling  $^{2S+1}[(^{2S^{(1)}+1}l_1^{N_1})(^{2S^{(2)}+1}l_2^{N_2})(^{2S^{(3)}+1}l_3^{N_3})]$  is described graphically by



where we have coupled (on the top part of the graph) the "1" electrons to the "3" electrons, giving a resultant spin  $S'$  and then coupled the "2" electrons to get the total spin  $S_N = S$ .

By breaking the graph part we see that within the "2" electron part of the graph we arrive once again at terms involving  $6-j$  symbols. Within the "3" part of the graph, however, we now find subgraphs of the form



where  $x_1$  and  $x_2$  assume all allowed values. The graph in (A8) can be rewritten as a  $9-j$  symbol.

In general, for  $t$  mixed-orbital configurations, we can expect the transformation coefficients between direct successive coupling modes and parent partition coupling modes to be  $3t-j$  coefficients for the  $t$ th pure configuration. In this sense then, the subduction coefficient method of PH is similar to the older Racah methods.

APPENDIX B: HIGHEST TABLEAUX AS EIGENFUNCTIONS OF  $L^2$

In Sec. IV it was asserted that any highest tableau  $|T\rangle$  is an eigenfunction of the  $L^2$  operator, that is,

$$L^2 |T\rangle = L_{\max}(L_{\max} + 1) |T\rangle. \tag{B1}$$

Thus  $|T\rangle$  uniquely defines a state

$$|^{(2S^{(1)}+1}l_1^{N_1}) \dots (^{2S^{(r)}+1}l_r^{N_r}) L_{\max} S M_L(\max) M_S \tau\rangle = |T\rangle. \tag{B2}$$

The operator  $L_\gamma$  is defined as the sum of operators for each pure configuration

$$L_\gamma = \sum_{i=1}^r L_\gamma^{(i)} \tag{B3}$$

and  $L_\gamma^{(i)}$  acts only on that part of the mixed orbital tableaux corresponding to the  $i$ th pure configuration, that is to say, there are no intershell operators. The values of  $\gamma = 0, +, -1$  correspond to measuring  $M_L^{(i)}$  or raising/lowering of the  $i$ th subtableau.

For each pure configuration highest tableau we have (viz., Fig. 2)

$$L_0^{(i)} |t^{(j)}\rangle = \delta_{ij} M_L^{(i)}(\max) |t^{(i)}\rangle, \tag{B4}$$

$$L_{-1}^{(i)} |t^{(j)}\rangle = -\left(\frac{a_{(i)}}{2} (2l_{(i)} + 1 - a_{(i)})\right)^{1/2} \delta_{ij} |t^{(i)'}\rangle - \left(\frac{(a_{(i)} + b_{(i)})}{2} (2l_{(i)} + 1 - a_{(i)} - b_{(i)})\right)^{1/2} \delta_{ij} |t^{(i)''}\rangle, \tag{B5}$$

$$L_{+1}^{(i)} |t^{(j)}\rangle = 0, \tag{B6}$$

where  $|t^{(i)'}\rangle$  and  $|t^{(i)''}\rangle$  are the resulting tableaux after lowering the lowest box in the right and left columns of  $|t^{(i)}\rangle$ , respectively. Operating on these lowered tableaux with  $L_{+1}^{(i)}$  gives back the highest tableau

$|t^{(i)}\rangle$  with the same eigenvalues, having opposite sign, as shown in (B5). Thus, for each highest tableau  $|t^{(i)}\rangle$  we find

$$\begin{aligned} L^{(i)2} |t^{(j)}\rangle &= (L_0^{(i)2} - L_{+1}^{(i)} L_{-1}^{(i)} - L_{-1}^{(i)} L_{+1}^{(i)}) |t^{(j)}\rangle \\ &= \delta_{ij} [M_L^{(i)}(\max)^2 + \frac{1}{2} a_{(i)} (2l_{(i)} + 1 - a_{(i)}) + \frac{1}{2} (a_{(i)} + b_{(i)}) (2l_{(i)} + 1 - a_{(i)} - b_{(i)})] |t^{(i)}\rangle \\ &= \delta_{ij} [M_L^{(i)}(\max)(M_L^{(i)}(\max) + 1)] |t^{(i)}\rangle, \end{aligned} \quad (\text{B7})$$

where we have used (2.3) to obtain the last line of (B7).

Expanding  $L^2$  in terms of  $L_\gamma^{(i)}$  we find, using (B4) and (B7),

$$\begin{aligned} L^2 |T; t^{(1)}, \dots, t^{(j)}, \dots, t^{(r)}\rangle &= \sum_{\gamma=1}^r (-1)^\gamma \sum_{i=1}^r L_\gamma^{(i)} \sum_{k=1}^r L_{-\gamma}^{(k)} |T; \dots t^{(j)} \dots\rangle \\ &= \left[ \sum_{i=1}^r L^{(i)2} + 2 \sum_{i \neq k} L_0^{(i)} L_0^{(k)} \right] |T; \dots t^{(j)} \dots\rangle \\ &= \left( \sum_{i=1}^r M_L^{(i)}(\max)(M_L^{(i)}(\max) + 1) + 2 \sum_{i \neq k} M_L^{(i)}(\max) M_L^{(k)}(\max) \right) |T; \dots t^{(j)} \dots\rangle \\ &= M_L(\max) [M_L(\max) + 1] |T; t^{(1)}, \dots, t^{(j)}, \dots, t^{(r)}\rangle \end{aligned} \quad (\text{B8})$$

where we have used (B3) in the final step. With  $L_{\max} = M_L(\max)$  we have proven our assertion.

<sup>1</sup>J. Drake, G. W. F. Drake, and M. Schlesinger, *J. Phys.* B 8, 1009 (1975).

<sup>2</sup>J. Paldus, *Phys. Rev. A* 14, 1620 (1976).

<sup>3</sup>G. W. F. Drake and M. Schlesinger, *Phys. Rev. A* 15, 1990 (1977).

<sup>4</sup>C. W. Patterson and W. G. Harter, *Phys. Rev. A* 15,

2372 (1977).

<sup>5</sup>D. M. Brink and G. R. Satchler, *Angular Momentum*, 2nd edition, (Clarendon, Oxford, 1968), Chap. VIII.

<sup>6</sup>R. D. Kent, M. Schlesinger, and G. W. F. Drake, *J. Comput. Phys.* (in press).